Phys. Rev. B, 92, 041407(R) (2015)

Controlling the electronic structure of graphene using surface-adsorbate interactions

Piotr Matyba, Adra V. Carr, Cong Chen, David L. Miller, Guowen Peng, Stefan Mathias, Manos Mavrikakis, Daniel S. Dessau, Mark W. Keller, Henry C. Kapteyn, and Margaret Murnane.

Department of Physics and JILA, University of Colorado and NIST, Boulder, Colorado 80309, United States

National Institute of Standards and Technology (NIST), 325 Broadway, Boulder, Colorado 80305, United States

Department of Physics and Research Center OPTIMAS, University of Kaiserslautern, 67663 Kaiserslautern, Germany

Department of Chemical and Biological Engineering, University of Wisconsin-Madison, Madison 53706, United States

Abstract

Hybridization of atomic orbitals in graphene on Ni(111) opens a large energy gap of ≈2.8 eV between non-hybridized states at the K-point. Here we use alkali metal adsorbate to reduce and even eliminate this energy gap, and also identify a mechanism responsible for decoupling graphene from the Ni substrate without intercalation of atomic species underneath graphene. Using angle-resolved photoemission spectroscopy and density functional theory calculations, we show that the energy gap is reduced to 1.3 eV due to moderate decoupling after adsorption of Na on top of graphene. Calculations confirm that after adsorption of Na the propensity of graphene bonding to Ni is much lower due to reduced overlap of atomic orbitals, which results from n-doping of graphene. Moreover, we show that the energy gap is eliminated by strong decoupling resulting in a quasi-freestanding graphene, which is achieved by subsequent intercalation of the Na underneath graphene. The ability to partially decouple graphene from a Ni substrate via n-doping (with or without intercalation) suggests that the graphene-to-substrate interaction could be controlled dynamically using light.

Graphene is a one-atom-thick sheet of carbon atoms that are arranged in a 2D honeycomb lattice. Its optical and electrical properties emerge from the linear dispersion of states near the K-point, which form a Dirac cone near the Fermi level [1]. This linear dispersion leads to excellent transport properties, including ballistic conductivity, massless charge carriers, and high charge carrier mobility [2-4]. However, graphene is sensitive to external perturbations such as interactions with the substrate or adsorbates, which can modify the energy of the Dirac cone through doping, or cause a band gap to open at the K-point due to symmetry breaking in the graphene sublattices [5-9].

Commensurate metal surfaces are excellent substrates for efficient growth of graphene through decomposition of gaseous precursors [10]. However, the strong coupling of the metal substrate is detrimental for the electronic properties of graphene [5]. In graphene grown on Ni(111) [Gr/Ni(111)] the states near the K-point hybridize with the metal states and split into multiple bands spanning the energy range from 0 eV down to 3 eV below the Fermi level [5, 11-13]. Although some of these bands intersect at the K-point forming band structures akin to the Dirac cone [14, 15], Gr/Ni(111) is metallic and this precludes its useful applications. It was shown that intercalants could weaken the coupling by forming an atomic spacer between graphene and the substrate [11-13, 16], but only noble metals were shown to effectively mitigate hybridization, making it possible to transfer graphene from Ni(111) onto different substrates and to employ it in devices [12, 17, 18].

Decoupling of the substrate by intercalation of noble metals underneath Gr/Ni(111) was used to produce quasi-freestanding graphene for spectroscopy and for device fabrication [12, 17, 18]. However, the role of alkali metal intercalants is still not clear. Although intercalated alkali atoms should detach graphene in a similar way to noble metals, providing charge and n-doping, work to date has resulted in severe inconsistencies. On one hand, intercalation of Na (and similarly K or Cs) was shown to reduce the energy gap between the non-hybridized states at the K-point (the π-to-π^* energy gap), from 2.8 eV to 1.3 eV [16, 19]. On the other hand, angle-resolved photoemission spectroscopy (ARPES) and density functional theory (DFT) showed that the energy gap is reduced to 0 eV after intercalation [15]. The origin of the large energy gap found in the previous experiments has not been addressed as-of-yet. While experiments have focused on the role of intercalation of atomic species underneath graphene, the effects of pure adsorption (i.e. adsorption not followed by intercalation) have been unnoticed. We note that adsorption of alkali metals onto graphene induce n-doping and was used to control the electronic structure in bi-layers of graphene on SiC(0001) [20]. Moreover, mechanisms of alkali metals intercalation of graphene were studied extensively using DFT, and scanning tunneling microscopy [21-26].

In this paper, we use ARPES to probe electronic states near the K-point during adsorption and subsequent intercalation of atomic Na into Gr/Ni(111). Changes in the dispersion of these states and the Fermi velocity in graphene are sensitive probes of the interactions with the substrate [27]. We use changes in the energy and dispersion of the π state at high momenta to examine the role of Na adsorption in decoupling graphene from the substrate. We identify two distinct regimes of decoupling, which were overlooked previously. First, we find that Na on top of graphene induces moderate decoupling from the substrate, which results in lowering the π-to-π^* energy gap from 2.8 eV to $\approx$1.3 eV, while also

changing the π state dispersion at high momenta. This decoupling was previously attributed to intercalation of Na (and K or Cs) into Gr/Ni(111) [16, 19]. Second, we show that proper annealing after adsorption leads to intercalation of the Na underneath graphene, which induces stronger decoupling and restores the almost pristine Dirac cone – thereby closing of the π-to-π* energy gap. Our experimental findings are confirmed by DFT band structure calculations and Bader charge analysis.

Ni(111) single crystal films were graphitized in UHV through dissociation of C_2H_4 (partial pressure of 10^{-6} Torr and Ni(111) temperature of 900 K) [10]. This monolayer of graphite was then dissolved into Ni(111) at temperatures >1100 K and subsequently precipitated onto the surface. The solubility of C in Ni is 3 times higher at 1100 K than at room temperature [28] and makes it possible to control the formation of graphene on the surface by slow cooling the sample [29]. Gr/Ni(111) formed at lower rates (ca. 2 hrs per monolayer), through precipitation of carbon rather than by direct dissociation of C_2H_4, showed the much better morphology that was critical for this study. Na was adsorbed under a pressure of $\approx 10^{-10}$ Torr at room temperature using a commercial Na source. Intercalation of Na was induced by annealing the sample at temperatures in the range of 300 to 450 K, followed by rapid cooling to room temperature.

ARPES was performed using 40.8 eV VUV radiation from a He discharge lamp (Specs UVS300) and a hemispherical analyzer (Specs Phoibos 100) [30]. The morphology of Gr/Ni(111) was examined using ARPES and low-energy electron diffraction (LEED). Intercalation of Na was diagnosed through exposures to O_2 in UHV, which results in oxidation of Na when on top of grapheme, but not when intercalated (due to the large size of the O_2 molecule [31]). DFT calculations were performed using the VASP code [32] based on spin-polarized DFT. The projector augmented wave potentials were used to model electron-ion interactions [33, 34] while Van der Waals dispersion forces were accounted for using the vdW-DF approach [32, 35-37] (more details in Supplementary Materials SM).

The band structure of Gr/Ni(111), measured experimentally along ΓK [12, 13, 16] and p-ΓK [14, 15] directions of the Brillouin zone, revealed that coupling to the substrate distorts the states near the K-point. In Fig. 1(a) we plot this band structure probed along the ΓK direction. The exact position of the K-point (Γ-point) is established from the minimum (minimum) the σ_3 state (π state). For the π state, we find that the maximum is lower in energy by ≈2.8 eV at the K-point then in graphene on SiC(0001), and that the minimum is also lower, but only by ≈2.0 eV at Γ. Since the energy "shifts" at Γ and K are not matched, we conclude that the state dispersion (i.e. dE/dk) along ΓK must be locally lower in Gr/Ni(111) than in graphene on SiC(0001), presumably due to coupling to the substrate (hybridization).

Theoretically, we find that the Ni d band spans from the Fermi level down to -3.5 eV along the entire cut through the Brillouin zone and close to the Γ-point it spans from -5 eV to -9 eV, as shown in Fig. 1(b). These higher binding energy states, which have been calculated previously [14], are not accessible in ARPES data due to matrix element effects. Notably, near the K-point this d band and the graphene π state intersect and hybridize [5, 14-16]. The extent of hybridization is lower near the Fermi level due a lower density of Ni(111) states. Therefore, we can identity remnants of the π state near the Fermi level in Fig. 1(b), and experimentally in Fig. 1(a) and in Fig. S1(b) in SM. We will see below that this state is influenced by adsorption and intercalation of Na.

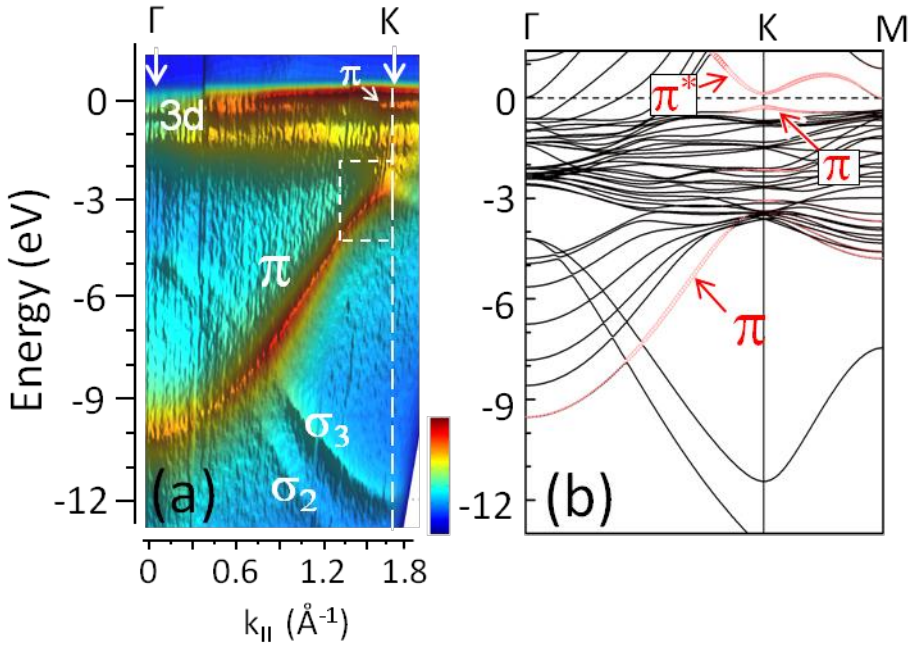

Fig. 1. (a) Electronic structure of pristine Gr/Ni(111) measured along the ΓK direction in the Brillouin zone; the π , σ_2 and σ_3 states of graphene and the 3d band of Ni(111) are indicated with symbols, while high symmetry points of the Brillouin zone (Γ, K) are indicated with vertical white arrows. (b) Calculated majority band structure of Gr/Ni(111). The graphene 2p_z contributions are highlighted in red.

The experimental spectrum in Fig. 1(a) clearly shows that the π state dispersion is lower in the momentum range from 1.4 Å^{-1} to 1.7 Å^{-1} (indicated as a white rectangle). This dispersion is influenced by coupling to the Ni states, which are strong in the corresponding energy range [down to -3 eV, in Fig. 1(b)]. In order to gain further insights into this coupling, we performed DFT calculations of the most stable (top-fcc) configuration, shown in Fig. 1(b). Our calculations omit the spectral weights or matrix elements relevant for ARPES, making it possible to show all important states along the ΓK direction (note that the experimental spectrum is dominated by the strongest spectral features). In the energy range down to -2.8 eV in Fig. 1(b), the d band and the π state are mixed and split into a dense manifold of states. The intensity of these hybridized states is low along the ΓK direction due to matrix element effects [38-40], which are induced by hybridization. Details of these states are not important for the arguments presented here. They were characterized previously using higher energy photons and/or other cuts through the Brillouin zone [14, 15].

Our DFT calculations in Fig. 1(b) show that the π* state is shifted in energy to above the Fermi level and that its dispersion is not linear near the K-point. We link this peculiar dispersion to the same hybridization that alters states below the Fermi level [in Figs. 1(a) and 1(b)] and we anticipate that this state will shift due to n-doping after adsorption of Na. Indeed, with 0.8 monolayer of Na on top, the π* state is slightly populated and shifted to below the Fermi level, as shown in Fig. 2(b). However, changes in the π state after adsorption cannot be explained as due to n-doping. That state maximum shows up at energy > -2.8 eV while the slope (dE/dk) is increased around the K-point, resulting in a lower π-to-π* energy

gap of ≈1.3 eV. Since n-doping should neither shift a populated state towards the Fermi level nor change the state dispersion, we conclude that these changes in Fig. 2(b) are due to a weaker coupling between graphene and the substrate after adsorption, and we validate these interpretations through theory below. We note that the π state is hybridized above -2.8 eV before adsorption in Fig. 2(a), and it is clearly restored in the energy window from -2.8 eV to ≈-1.3 eV after adsorption in Fig. 2(b).

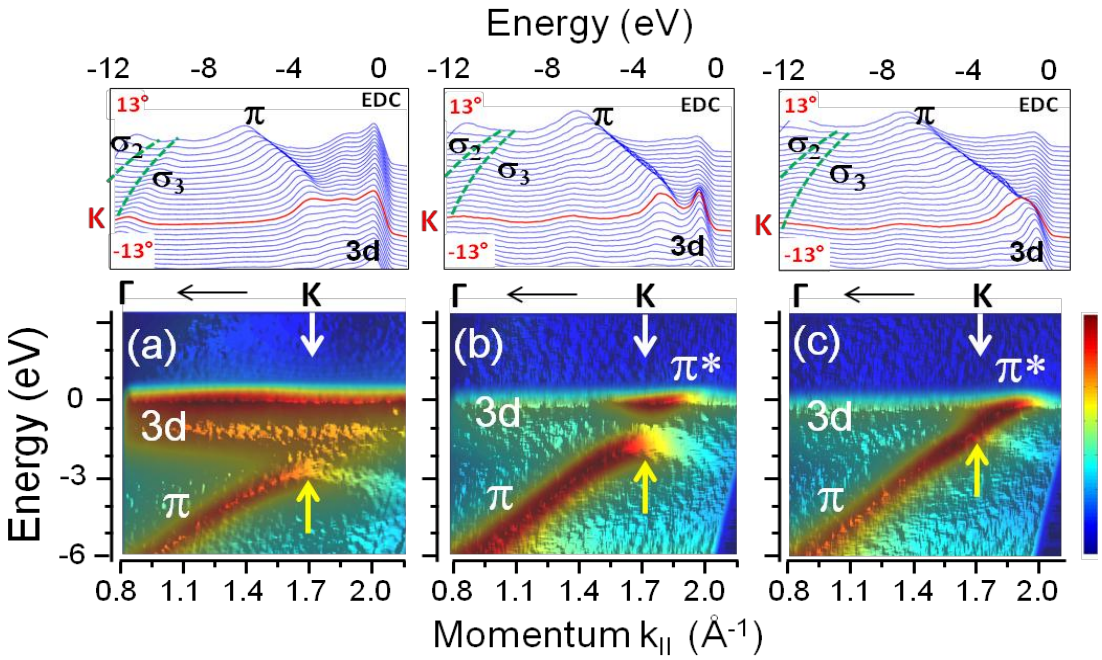

Fig. 2. (a) Experimental band structure of graphene on Ni(111), where the K-point is indicated by vertical white arrows (↓). The insets above show the energy distribution curves (EDCs) near the K-point (the K-point EDC is indicated in red) as a function of detection angle. The EDCs energy range is from -12 eV to 1 eV. (b) Same as (a) but after adsorption of 0.8 monolayer Na on top; the minimum of the π* state is visible at the Fermi level. The yellow vertical arrows (↑) indicate roughly the maximum of the π state, established from the state turning point. (c) Same as (b) after further annealing to intercalate Na to underneath graphene.

Previous studies, which observed a lowering of the π-to-π* energy gap to 1.3 eV after adsorption of Na (or K and Cs) onto Gr/Ni(111), overlooked changes in the dispersion of the π state near the K-point [16, 19]. The lowering of the energy gap was attributed to intercalation of Na (K, Cs) into graphene, although no proof of intercalation was shown. In contrast, our experimental results (supported by DFT calculations) exclude intercalation as the origin of changes observed in Fig. 2(b). We further confirmed that the Na atoms remain on top of graphene by exposing the sample to O_2 in UHV. Since Na is prone to oxidation, this gives rise to photoemission lines from sodium oxides [41] (see SM). We also exclude intercalation in isolated areas leading to islands of decoupled and still-coupled graphene. Such decoupling was shown to produce a superposition of two π states, one from intercalated and one from non-intercalated areas [15], which we do not observe here. We also emphasize that angle-resolved or angle-integrated XPS measurements cannot confirm intercalation of Na into graphene. Changes in the intensity of XPS lines from a monolayer of Na (K, Cs) adsorbed on graphene are often due to formation of thick islands of adsorbates on top, rather than intercalation [23, 31, 42].

Figures 3(b) and 3(c) plot the calculated electronic structures of Gr/Ni(111) both without Na, and with Na on top, respectively. The hybridized π* state above the Fermi level and the remnants of the π state below the Fermi level are shifted down in energy after adsorption, as shown in Fig. 3(b) [note that energy is referenced to the Fermi level in Figs. 3(a)-(d)]. Since the Fermi level is shifted upwards after adsorption (due to n-doping), it is expected that all other states in Fig. 3(c) shift down compared to Fig. 3(b). However, the hybridized states below the Fermi level remain fixed throughout and after adsorption, which we link to a screening effects associated with charge density rearrangements. We note that the spectral intensity of these hybridized states is strongly diminished after adsorption, as seen in Fig. 2(b), suggesting that the extent of hybridization is reduced after adsorption, which we further investigate below [43].

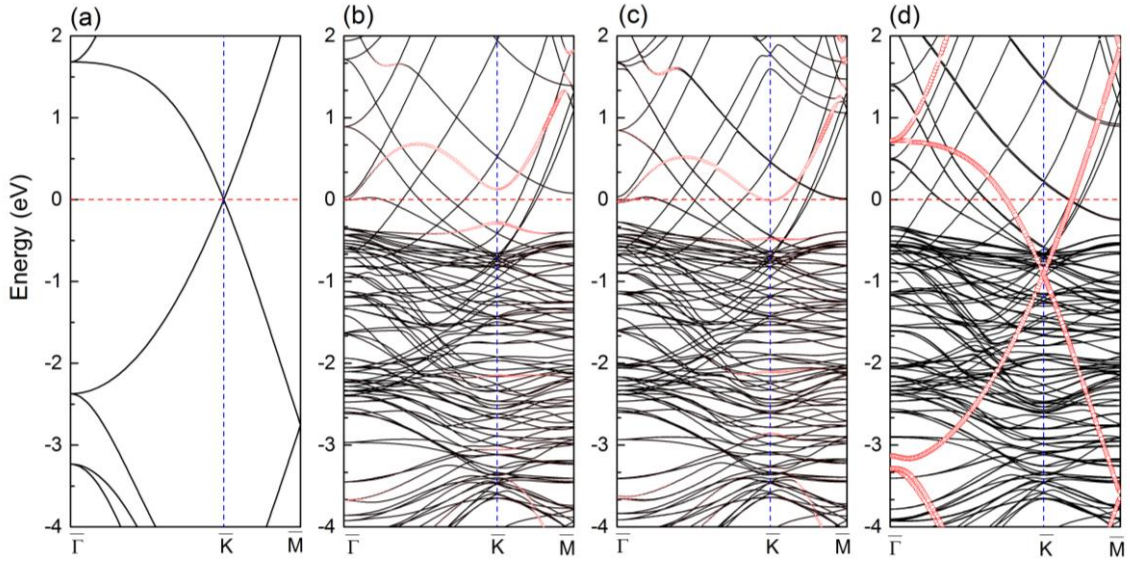

Fig. 3. Band structures for (a) freestanding graphene, (b) Gr/Ni(111), (c) Na/Gr/Ni(111), and (d) Gr/Na/Ni(111) in a (2×2) supercell, corresponding to a Na coverage of 0.75 ML. The contributions of graphene $2p_z$ states are highlighted in red in panels (b)-(d).

The plots of the charge density difference before and after adsorption are shown in Figs. 4(a) and 4(b), to give a more physical intuition about nature of the decoupling. In Gr/Ni(111), the atomic orbitals of graphene ($2p_z$) and Ni(111) ($3d_{3z^2-r^2}$) overlap at the substrate top-sites, giving rise to a strong chemical bond and the concomitant charge density redistribution shown in Fig. 3(a). The Bader charge analysis shows that, in the energetically most stable arrangement, these orbitals are hybridized and a net charge of 0.10 e (e is the elementary charge) is transferred to graphene. The charge rearrangement before adsorption involves predominantly the $2p_z$ and $3d_{3z^2-r^2}$ atomic orbitals and other orbitals are not involved. After adsorption, this charge redistribution and the associated energetics shift because of the electrons supplied to graphene by Na. The Bader charge analysis shows that Na adsorption brings a net charge of 0.36 e per atom to graphene and no charge to the substrate, causing an interfacial dipole causing lifting graphene slightly off the substrate. Our DFT calculations show that graphene receives only 0.05 e per atom from the substrate after adsorption, i.e. only a half of the charge received before adsorption. This is due to a weaker overlap of the atomic orbitals and the energetics that favor graphene receiving the charge from Na rather than sharing it with Ni(111). The consequence of adsorption of Na on top is that the structure of Gr/Ni(111) is slightly relaxed and the layer of graphene is lifted up to 2.30 Å above the

substrate. Although the detailed energetics are complex, we conclude that graphene must decouple from the substrate after strong n-doping in order to minimize the energy. We also anticipate that a higher charge transfer per atom from the adsorbate would yield even stronger decoupling, which is consistent with previous measurements on Gr/Ni(111) [19].

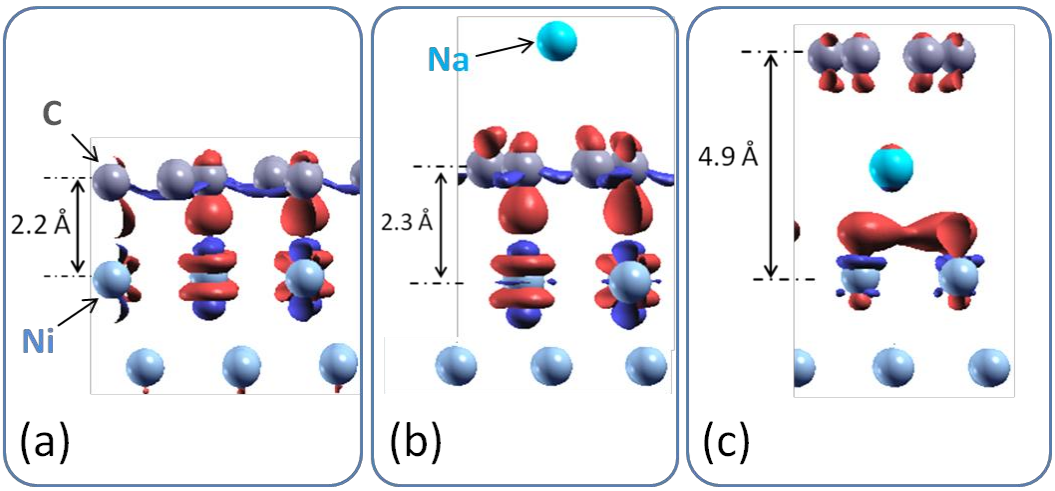

Fig. 4. Charge density difference plots, using an isosurface of ±0.02 e/Å^3 for (a) Gr/Ni(111), (b) Na/Gr/Ni(111), and (c) Gr/Na/Ni(111); charge density accumulation is shown in red and depletion in blue. The adsorption energy of Na on Gr/Ni is -1.00 eV at a Na coverage of 1 ML, referenced to the total energies of atomic Na and Gr/Ni(111).

We emphasize that this decoupling induced by Na on top involves a notably different mechanism than decoupling through intercalation of noble metals into Gr/Ni(111), which was investigated extensively in the past [8, 9, 11, 12, 31]. Bulky atoms break down hybridization at the graphene-substrate interface, resulting in detaching graphene from the substrate and lowering the energy gap between non-hybridized states at the K-point. When an electron-donating adsorbate remains on top of graphene, the energetics are changed, inducing relaxation of the bonding at the graphene-substrate interface, although graphene is not detached from the substrate.

Since results from previous experiments on alkali metal intercalants in Gr/Ni(111) are ambiguous, showing ≈1.3 eV gap opening after intercalation [16, 19] or gap closing [15] under identical conditions, we performed intercalation of Na with the sample held in front of the photoelectron detector at the same position as in Fig. 2(b) to resolve this inconsistency, [shown in Fig. 2(c), see the discussion of intercalation in SM]. We find that the energy gap is reduced to ≈0 eV and the Dirac cone is restored after intercalation. In addition, the Fermi velocity, which serves us a gauge of the coupling to the substrate [27], is increased after intercalation towards the value of freestanding graphene (≈1.6×10^6 m/s), indicating decoupling.

We further confirm this by analyzing the corresponding charge density differences in Fig. 4(c), which show that graphene is lifted up to 4.9 Å above the substrate and is cut-off from the substrate, and the band structure in Fig. 3(d). The hybridization is blocked by an atomic spacer of Na and thus there is only a weak or absent energy gap at the K-point. We expect that the remnant gap opening (<≈100 meV) or the minor band back-bending seen in Fig. 2(c) is a result of superposition of regions with complete inter-

calated and regions where Na still remains on top. This is reasonable due to the supply of Na (0.8 monolayers) and possibly some bottlenecks in the intercalation paths. Our experiments and DFT calculations show thus that intercalation of Na is nearly the same in its effect as intercalation of noble metals, although strong n-doping is concurrent with decoupling.

Although recent experiments suggested that Na may intercalate spontaneously due to the low energy barrier [15], we do not observe spontaneous intercalation at room temperature. Instead, we find that intercalation is not possible unless graphene features defects or grain boundaries (which is expected due to the size of atomic Na) and unless the mobility of Na is increased by temperature. Our DFT calculations further support this observation. Although the arrangement with Na on top is not optimal from the energetics standpoint, and the adsorbate tends to intercalate, the intercalation is kinetically limited without grain boundaries and defects. Our intercalation study on a high number of Gr/Ni(111) samples grown under different conditions, in which we were able to achieve relatively good control over the concentration of defects in graphene by introducing oxide impurities into the Ni(111) substrate and by performing the growth at lower temperatures producing impurities of amorphous carbon [44], shows that intercalation of Na is indeed morphology dependent. When graphene shows relatively weak spectral features in ARPES and LEED, with a high background of secondary electrons, intercalation is possible at lower temperatures. Intercalation into a higher quality graphene sheet requires elevated temperatures and intercalation into the highest quality graphene needs temperatures close to the desorption threshold.

In summary, we show that the presence of Na atoms on top of Gr/Ni(111) induce decoupling of graphene from the substrate, as evident from a decrease of the π-to-π* energy gap to 1.3 eV. Moreover, intercalation of Na underneath graphene recovers near-pristine graphene, closing this energy gap to near 0 eV. We anticipate that the mechanism of controlling the extent of graphene-to-substrate coupling using a charge transfer from adsorbates, rather than intercalation, opens new possibilities in using optical (laser) excitations to control this coupling in graphene on other surfaces. This technique might allow for switching the graphene-to-substrate coupling in the spirit of previous work on noble metal surfaces and alkali metal adsorbates; cf. references [45, 46].

The authors gratefully acknowledge support from the National Science Foundation Physics Frontiers Center Program. DD acknowledges support from grant DOE-BES DE-FG02-03ER46066. PM acknowledges fellowship from the Swedish Research Council (Vetenskapsrådet). Work at UW was partially supported by Department of Energy-Basic Energy Sciences (DOE-BES) and by the Air Force Office of Scientific Research under Basic Research Initiative grant AFOSR FA9550-12-1-0481. The computational work was performed in part using supercomputing resources from the following institutions: EMSL, a National scientific user facility at Pacific Northwest National Laboratory (PNNL); the Center for Nanoscale Materials (CNM) at Argonne National Laboratory (ANL); and the National Energy Research Scientific Computing Center (NERSC). EMSL is sponsored by the Department of Energy's Office of Biological and Environmental Research located at PNNL. CNM and NERSC are supported by the U.S. Department of Energy, Office of Science, under Contracts DE-AC02-06CH11357 and DE-AC02-05CH11231, respectively.

References

1. Geim, A.K. and K.S. Novoselov, *The rise of graphene.* Nature Materials, 2007. **6**(3): p. 183-191.

2. Zou, K., X. Hong, and J. Zhu, *Effective mass of electrons and holes in bilayer graphene: Electron-hole asymmetry and electron-electron interaction.* Physical Review B, 2011. **84**(8).

3. Novoselov, K.S., et al., *Two-dimensional gas of massless Dirac fermions in graphene.* Nature, 2005. **438**(7065): p. 197-200.

4. Bolotin, K.I., et al., *Ultrahigh electron mobility in suspended graphene.* Solid State Communications, 2008. **146**(9-10): p. 351-355.

5. Voloshina, E. and Y. Dedkov, *Graphene on metallic surfaces: problems and perspectives.* Physical Chemistry Chemical Physics, 2012. **14**(39): p. 13502-13514.

6. Papagno, M., et al., *Large Band Gap Opening between Graphene Dirac Cones Induced by Na Adsorption onto an Ir Superlattice.* Acs Nano, 2012. **6**(1): p. 199-204.

7. Walter, A.L., et al., *Electronic structure of graphene on single-crystal copper substrates.* Physical Review B, 2011. **84**(19): p. 195443-195443.

8. Amft, M., et al., *Adsorption of Cu, Ag, and Au atoms on graphene including van der Waals interactions.* Journal of Physics-Condensed Matter, 2011. **23**(39): p. 395001-395011.

9. Ren, Y.J., et al., *Controlling the electrical transport properties of graphene by in situ metal deposition.* Applied Physics Letters, 2010. **97**(5): p. 053107-05310.

10. Miller, D.L., et al., *Epitaxial (111) films of Cu, Ni, and CuxNiy on alpha-Al2O3 (0001) for graphene growth by chemical vapor deposition.* Journal of Applied Physics, 2012. **112**(6): p. 064317-064319.

11. Varykhalov, A., et al., *Electronic and Magnetic Properties of Quasifreestanding Graphene on Ni.* Physical Review Letters, 2008. **101**(15): p. 066804-066808.

12. Varykhalov, A., et al., *Effect of noble-metal contacts on doping and band gap of graphene.* Physical Review B, 2010. **82**(12): p. 121101-121105.

13. Haberer, D., et al., *Tunable Band Gap in Hydrogenated Quasi-Free-Standing Graphene.* Nano Letters, 2010. **10**(9): p. 3360-3366.

14. Varykhalov, A., et al., *Intact Dirac Cones at Broken Sublattice Symmetry: Photoemission Study of Graphene on Ni and Co.* Physical Review X, 2012. **2**(4): p. 041017-041027.

15. Park, Y.S., et al., *Quasi-Free-Standing Graphene Monolayer on a Ni Crystal through Spontaneous Na Intercalation.* Physical Review X, 2014. **4**(4): p. 031016-031025.

16. Gruneis, A. and D.V. Vyalikh, *Tunable hybridization between electronic states of graphene and a metal surface.* Physical Review B, 2008. **77**(19): p. 193401-193401.

17. Reina, A., et al., *Layer Area, Few-Layer Graphene Films on Arbitrary Substrates by Chemical Vapor Deposition.* Nano Letters, 2009. **9**(8): p. 3087-3087.

18. Regan, W., et al., *A direct transfer of layer-area graphene.* Applied Physics Letters, 2010. **96**(11).

19. Nagashima, A., N. Tejima, and C. Oshima, *Electronic States of the Pristine and Alkali-Metal-Intercalated Monolayer Graphite/Ni(111) Systems.* Physical Review B, 1994. **50**(23): p. 17487-17495.

20. Ohta, T., et al., *Controlling the electronic structure of bilayer graphene.* Science, 2006. **313**(5789): p. 951-954.

21. Petrovic, M., et al., *The mechanism of caesium intercalation of graphene.* Nature Communications, 2013. **4**.

22. Chakarov, D.V., et al., *Photostimulated Desorption of Metal Adatoms - Potassium on Graphite.* Surface Science, 1994. **311**(3): p. L724-L730.

23. Watcharinyanon, S., et al., *Changes in structural and electronic properties of graphene grown on 6H-SiC(0001) induced by Na deposition.* Journal of Applied Physics, 2012. **111**(8): p. 083711-083717.

24. Boukhvalov, D.W. and C. Virojanadara, *Penetration of alkali atoms throughout a graphene membrane: theoretical modeling.* Nanoscale, 2012. **4**(5): p. 1749-1753.

25. Li, Y.C., et al., *Lithium Intercalation Induced Decoupling of Epitaxial Graphene on SiC(0001): Electronic Property and Dynamic Process.* Journal of Physical Chemistry C, 2011. **115**(48): p. 23992-23997.

26. Choi, S.M. and S.H. Jhi, *Electronic property of Na-doped epitaxial graphenes on SiC.* Applied Physics Letters, 2009. **94**(15).

27. Hwang, C., et al., *Fermi velocity engineering in graphene by substrate modification.* Scientific Reports, 2012. **2**: p. 590-594.

28. Dunn, W.W., R.B. McLellan, and W.A. Oates, *SOLUBILITY OF CARBON IN COBALT AND NICKEL.* Transactions of the Metallurgical Society of America, 1968. **242**(10): p. 2129.

29. Zhang, Y., L. Zhang, and C. Zhou, *Review of chemical vapor deposition of graphene and related applications.* Acc Chem Res, 2013. **46**(10): p. 2329-39.

30. Equipment is identified in this paper only in order to adequately specify the experimental procedure. Such identification does not imply endorsement by the National Institute of Standards and Technology (NIST), nor does it imply that the equipment identified is the best available for the purpose.

31. Dedkov, Y.S., et al., *Graphene-protected iron layer on Ni(111).* Applied Physics Letters, 2008. **93**(2): p. 022509-022513.

32. Kresse, G. and J. Furthmüller, *Efficient iterative schemes for ab initio total-energy calculations using a plane-wave basis set.* Phys. Rev. B, 1996. **54**: p. 11169-11186.

33. Blochl, P.E., *PROJECTOR AUGMENTED-WAVE METHOD.* Physical Review B, 1994. **50**(24): p. 17953-17979.

34. Kresse, G. and D. Joubert, *From ultrasoft pseudopotentials to the projector augmented-wave method.* Physical Review B, 1999. **59**(3): p. 1758-1775.

35. Dion, M., et al., *Van der Waals density functional for general geometries.* Physical Review Letters, 2004. **92**(24): p. 246401-246405.

36. Klimes, J., D.R. Bowler, and A. Michaelides, *Chemical accuracy for the van der Waals density functional.* Journal of Physics-Condensed Matter, 2010. **22**(2): p. 022201-022206.

37. Klimes, J., D.R. Bowler, and A. Michaelides, *Van der Waals density functionals applied to solids.* Physical Review B, 2011. **83**: p. 195131-195144.

38. Mulazzi, M., et al., *Matrix element effects in angle-resolved valence band photoemission with polarized light from the Ni(111) surface.* Physical Review B, 2006. **74**(3).

39. Haarlammert, T., et al., *Final-state effects in photoemission experiments from graphene on Ni(111).* European Physical Journal B, 2013. **86**(5).

40. Hüfner, S., *Photoelectron spectroscopy : principles and applications*. Springer series in solid-state sciences 82. 1995, Berlin ; New York: Springer-Verlag. xii, 511 p.

41. Shek, M.L., et al., *Interaction of Oxygen with Sodium at 80-K and 20-K.* Physical Review B, 1986. **34**(6): p. 3741-3749.

42. Sandin, A., et al., *Multiple coexisting intercalation structures of sodium in epitaxial graphene-SiC interfaces.* Physical Review B, 2012. **85**(12): p. 125410-124115.

43. A sub-monolayer of adsorbate should not diminish significantly the spectral intensity of the underlying layer.

44. Gamo, Y., et al., *Atomic structure of monolayer graphite formed on Ni(111).* Surface Science, 1997. **374**(1-3): p. 61-64.

45. Sandell, A., et al., *Bonding of an isolated K atom to a surface: Experiment and theory.* Physical Review Letters, 1997. **78**(26): p. 4994-4997.

46. Watanabe, K., N. Takagi, and Y. Matsumoto, *Direct time-domain observation of ultrafast dephasing in adsorbate-substrate vibration under the influence of a hot electron bath: Cs adatoms on Pt(111).* Physical Review Letters, 2004. **92**(5): p. 057401-057405.